



**HAL**  
open science

# Mixing across a density interface in a Taylor-Couette flow

Estelle Guyez, Jan-Bert Flór, Emil J. Hopfinger

► **To cite this version:**

Estelle Guyez, Jan-Bert Flór, Emil J. Hopfinger. Mixing across a density interface in a Taylor-Couette flow. ISSF international Symposium on Stratified Fluid, Dec 2006, Perth, Australia. hal-00207211

**HAL Id: hal-00207211**

**<https://hal.science/hal-00207211>**

Submitted on 14 Apr 2020

**HAL** is a multi-disciplinary open access archive for the deposit and dissemination of scientific research documents, whether they are published or not. The documents may come from teaching and research institutions in France or abroad, or from public or private research centers.

L'archive ouverte pluridisciplinaire **HAL**, est destinée au dépôt et à la diffusion de documents scientifiques de niveau recherche, publiés ou non, émanant des établissements d'enseignement et de recherche français ou étrangers, des laboratoires publics ou privés.



Distributed under a Creative Commons Attribution 4.0 International License

# Mixing across a density interface in a Taylor-Couette flow

E. Guyez, J.-B. Flór & E. Hopfinger

LEGI-CNRS, BP 53X, 38041 Grenoble cedex 09, France  
flor@hmg.inpg.fr hopfinger@hmg.inpg.fr

## Abstract

In this paper we report on an experimental investigation of the interfacial mixing by Taylor vortices. Using the LIF method the evolution of the density field is followed in time for a range of buoyancy frequencies and Reynolds numbers. It is found that the buoyancy flux, represented as a function of the buoyancy gradient, shows a similar tendency as the mixing in isotropic turbulent flows. New is the increase in buoyancy flux for very large buoyancy gradients, predicted by the model of Balmforth et al. (1998). Since shear instabilities are unlikely to occur, other changes in the mixing processes should be responsible. In addition a spread in the maximum mixing efficiency is found, which is dependent on Reynolds number. The origins of this Reynolds number dependence, as well as the application of the mixing results to Langmuir Circulation in the ocean thermocline are discussed.

## 1. Introduction

Mixing of the upper ocean layer due to shear instability, internal wave breaking, convection *e.g.* due to evaporation of salt water and Langmuir vortices, concerns a long standing issue in fluid mechanics (see Thorpe, 2004b). The relevance of Langmuir Circulation (below abbreviated as LC) to upper ocean mixing has been subject to recent debates. Observations have confirmed the importance of LC in layer deepening, but to which extent these contribute in comparison to other mixing mechanisms has not been clarified (Thorpe, 2004a). Li et al. (2005) classify the different upper ocean eddies and reveal that, for a typical ocean state condition, the vertical velocity in LC is about 2 times that due to the shear turbulence, implying the dominance of Langmuir turbulence for the mixing dynamics of the upper ocean. Motivated by the application of ocean mixing, we consider the mixing of an interface by horizontal vortices, driven by the centrifugal force in a Taylor Couette device.

Former experimental investigations on mixing consider isotropic grid-generated turbulence, shear-driven turbulence or locally generated turbulence as forcing mechanism (Fernando, 1991). The mixing evolution is often represented in an asymmetric bell shaped curve, representing the buoyancy flux as a function of the buoyancy gradient: for low buoyancy gradients, the flux is proportional to the gradient up to a maximum buoyancy flux, beyond which stratification hinders vertical transport and mixed layers form, separated by sharp interfaces. This evolution is found conform to most experimental observations and in agreement with the well known theoretical model of Phillips (1971) and Posmentier (1977). The failure of this model is that it predicts, for large buoyancy fluxes, an unlimited sharpening of interfaces when neglecting molecular diffusion. Balmforth et al. (1998) eliminate this singularity in proposing a model that includes turbulent eddy diffusion of kinetic energy and of buoyancy, while taking a buoyancy dependent mixing length. When the buoyancy gradient increases, the kinetic energy is injected at smaller and smaller scales, thus resulting in a smaller mixing length and hence a more efficient

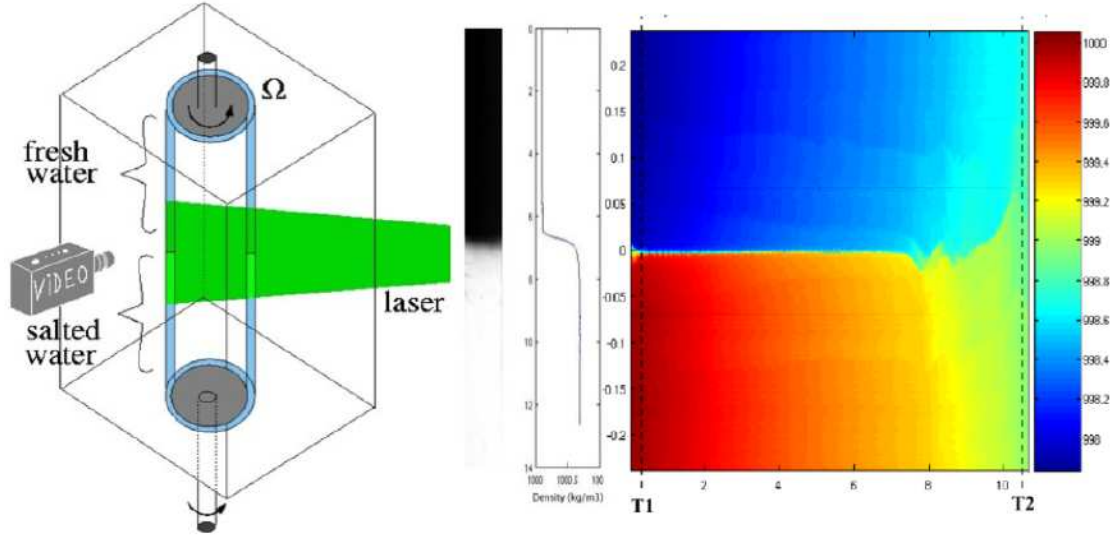


Figure 1: (a) Sketch of the experimental setup with the gap containing dyed salty water, the position of the laser sheet, and a measurement of the initial density profile of a diffused interface. (b) Typical spatio-temporal evolution of the averaged density profile in the gap; the color map at the right gives the density scale.

entrainment. As a consequence, the asymmetric bell-shaped model-curve changes to an N-shaped curve, with the flux increasing again at large buoyancy gradients. This increase in buoyancy flux at high  $Ri$ -number has never been observed in experiments before.

## 2. Experimental device and measurements

Two different Taylor-Couette devices are employed, one of the classical type with a thin gap of  $d=1$  cm and height to gap-width ratio of 56 and inner radius  $a=5$  cm (small TC-device), and a more unconventional one with  $d=5$  cm of ratio 12.4 and inner radius  $r=15$  cm (large TC device) used before by Boubnov et al. (1995) and Boubnov and Hopfinger (1997) for the study of on the effect of linear stratifications on stability regimes and vortex structures. The Reynolds number,  $Re = \Omega ad/\nu$  (with cylinder rotation frequency  $\Omega$ ) ranged from 100 and 4000. A sketch of the experimental setup and a typical density profile are presented in figure 1.

The initial density interface thickness was about 2 cm and the initial buoyancy difference was  $0.006 < \Delta B_i < 1.32$  cm s<sup>-2</sup> ( $\Delta B = g\Delta\rho/\bar{\rho}$ ) with  $\Delta\rho$  and  $\bar{\rho}$  respectively the density difference and mean density, and  $g$  the gravity constant. A known concentration of fluorescent dye ( $10^{-6}$  mol/l of Rhodamine 6G) was diluted in the lower dense layer, and illuminated by a 5 W argon laser. Using a 1000x1000 pixel B&W 8 bit CCD-camera the dye concentration was followed in time over a cross section of the gap with the LIF method. A resolution of 1% of the initial dye concentration, as well as a closely comparable accuracy in the density measurements, was achieved. For the density profiles, an average was defined over the gap width, and one rotation turn of the inner cylinder.

Turbulent eddy velocities were measured with a frequency of 10 times the rotation frequency of the inner cylinder, using the PIV method and algorithm developed by Fincham and Delerce (2000). Slightly heavy particles were seeded in the fluid which remained

equally distributed over the entire fluid depth for approximately 2 hours.

The buoyancy flux and buoyancy gradient, which characterize the mixing, are generally represented in the nondimensional form of the Richardson flux number versus Richardson number. Here, the buoyancy flux and buoyancy gradients are made dimensionless by the kinetic energy input proportional to the rms eddy velocity  $U_\vartheta$  of a Taylor-vortex of size  $d_\vartheta$ . The rms velocity has been obtained from PIV measurements. For a Reynolds number  $Re = 3407$  and  $d_\vartheta(t) = (h - z_m(t))/6 \approx 5$  cm,  $U_\vartheta = 0.76$  cm s<sup>-1</sup>. The instantaneous Richardson number, is then

$$Ri_o(t) = \frac{d_\vartheta(t)\Delta B(t)}{U_\vartheta^2} \quad (1)$$

and its value is known from the experiments with the direct measurements of  $\Delta B(t) = g\Delta\rho(t)/\bar{\rho}$ . The buoyancy flux is measured from the temporal evolution in the dye concentration which is proportional to the density and is given by the integral

$$F(z, t) = \int_z^h \frac{\partial\rho(z, t)}{\partial t} dz. \quad (2)$$

We suppose that the entrainment velocity above the interface is not affected by the mixing below the interface (Turner, 1968). The flux is zero at the boundaries  $z = 0$  and  $z = h$  whereas at the interface the flux is

$$F(z_m, t) = \Delta\rho(t)U_e(t) \quad (3)$$

where  $U_e$  is the entrainment velocity across the interface. The density difference,  $\Delta\rho$ , varies in each experiment from the initial value  $\Delta\rho_i$  to zero at the end of the experiment. The integration is from the interface  $z_m$ , defined by the mean density level, to the surface  $h$ . The entrainment coefficient is of the form

$$E(t) = \frac{U_e(t)}{U_\vartheta} \quad (4)$$

and Richardson flux number is given by  $Ri_f = Ri_o(t)E(t)$ . With the values of  $F(z_m, t)$  and  $\Delta\rho(t)$  measured from the experiments, the values of  $E$  and  $Ri_f$  are known.

### 3. Results and discussion

For the constant Reynolds number case ( $Re = 3409$ ) and large  $Ri_o$ , we found that the curves  $E$  as a function of  $Ri_o$  generally have a slope close to  $Ri_o^k$  with  $k = 1.32$ , whereas in the limit of small  $Ri_o < 10$ , the entrainment rate was found to vary between  $10^{-2}$  and  $3.10^{-2}$  (graph not shown here). This slope as well as the entrainment coefficient are close to the values found for the mixing in isotropic turbulence (Fernando, 1991). For  $Ri_o > 10$  differences in  $E$  could be noticed; this difference is clearly seen in the buoyancy flux- gradient relation shown in figure 2. For  $Ri_o > 100$ , figure 2 shows that the mixing efficiency flattens out and even increases with  $Ri_o$ . This increase is not related to the initial sharpening of the interface but to a change in mixing mechanism.

The increase in mixing efficiency at large buoyancy gradients should be associated with a change in mixing mechanism. Going from small to larger  $Ri_o$ , the Taylor vortices scrape the interface up till the minimum  $Ri_f$ , and show for larger  $Ri_o$  small scale overturning events (see images in figure 2). The origin of these overturning events is not yet

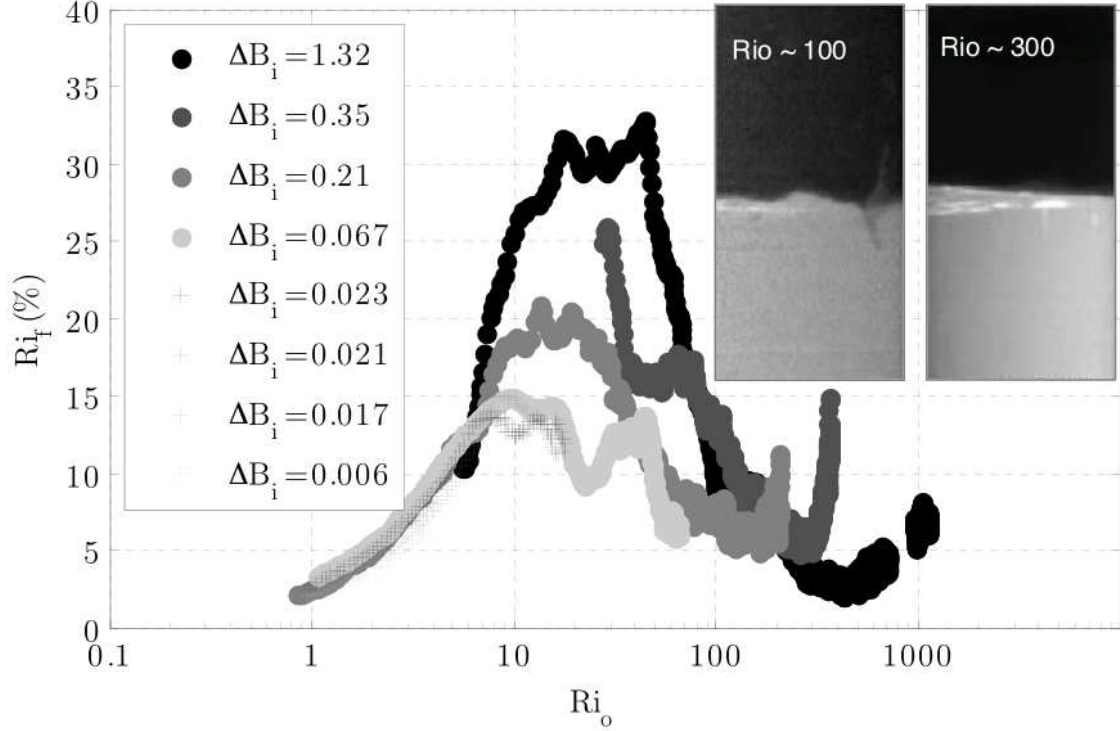


Figure 2: *Mixing efficiency  $Ri_f$  presented as a function of the Ri-number  $Ri_o$ , for a constant Reynolds number  $Re = 3409$  and various  $\Delta B$  (see legend). The images represent the flow before and after the increase in mixing efficiency;  $\Delta B = 0.35 \text{ m.s}^{-2}$ .*

understood.

Another interesting result of the present investigation is the variation of the maximum mixing efficiency with Reynolds number, which shows a maximum for a specific Reynolds number (see figure 3a). This tendency in mixing efficiency can equally be recognized in the total mixing efficiency (see fig. 3b),  $\bar{Ri}_f = \Delta P / \Delta E$ , where the total kinetic energy required to mix the two-layer fluid in time  $T_2$  (fig. 1b) is estimated as  $\Delta E = M\Omega T_2$ , where  $M$  is the torque acting on the inner rotating cylinder and  $\Delta P = V\Delta B\bar{\rho}h/2$ , with  $V$  the volume of the gap (Ermanyuk and Flór, 2005). In Taylor Couette flows, the flow structure varies with Reynolds number and, to a minor extent, with stratification in a two-layer stratified fluid. Though the exact flow details need further investigations, this suggests that the highest mixing efficiency is not ruled by turbulence intensity, but by the particular flow structure. Both, the increase in mixing efficiency for very large  $Ri_o$  numbers Guyez et al. (2006), as well as the tendency of the Richardson flux number with Reynolds number have not been observed before.

The Taylor vortex flow that mixes the density interface in the TC device has many similarities with the Langmuir circulation which interacts with oceanic pycnocline; both have horizontal vortex axis. The symmetry plane of the Langmuir vortices is in the Taylor-Couette flow replaced by the cylinder wall. Li et al. (1995) have established a criteria which stipulates that the deepening of the surface layer due to LC is inhibited when  $Ri_o > 12$ . In the TC experiments, this is the limiting value beyond which the entrainment rate is no longer constant and starts to decrease very rapidly. Thus, the depth of the oceanic surface layer can be considered to remain nearly constant when  $Ri_o > 12$ . In the TC experiments

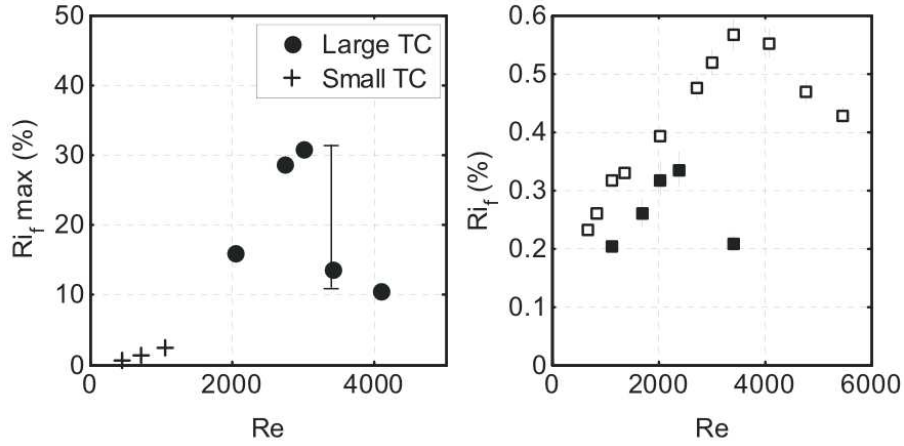


Figure 3: a) Maximum mixing efficiency  $Ri_f$  of the TC flow as a function of the overall Re-number. The vertical line represents the relatively large error which is due to the large variation in maximum mixing efficiency (see figure 2); b) Total mixing efficiency as measured for the total mixing of the interface.

the non-dimensional entrainment rate  $E$  for  $Ri_0 < 12$  is  $10^{-2}$ , a value comparable with those measured for LC mixing during a storm event. Smith (1998) finds an entrainment velocity  $U_e \approx 0.14 \text{ mm s}^{-1}$  which with the rms velocity  $U_{rms} \approx 1.5 \text{ cm s}^{-1}$  in LC cells yields a very comparable non-dimensional entrainment rate.

#### 4. Conclusions

Mixed layer deepening by Taylor vortices has similarities with mixing of the ocean surface layer by Langmuir circulation. It is shown that the Froude number criterion given by Li and Garrett (1997) for the arrest of mixed layer deepening by LC cells corresponds to conditions where the mixing rate starts to decrease rapidly. Concerning the physics of mixing, the experiments of mixing by Taylor vortices exhibit two novel features. One is the flattening and increase in mixing efficiency at large Richardson numbers, predicted by the model of Balmforth et al. (1998) and the other is the considerable variability in the flux-gradient relation. The reason for this variability is not clear but it is likely to be a consequence of intermittent mixing events occurring at a slow time scale compared with the eddy turnover time. It is further shown that mixing depends on Reynolds number with maximum mixing at an eddy Reynolds number of about 3000.

#### Acknowledgements

E. Guyez acknowledges a DGA fellowship. This work has been supported by SHOM grant  $n^o$ : 02.87.028.00.470.29.25.

## References

- Balmforth, N. J., Llewellyn Smith, S. G., and Young, W. R. (1998). Dynamics of interfaces and layers in a stratified turbulent fluid. *J. Fluid Mech.*, 428:349–386.
- Boubnov, B. M., Gledzer, E., and Hopfinger, E. J. (1995). Stratified circular Couette flow: instability and flow regimes. *Journal of Fluid Mechanics*, 292:333–358.
- Boubnov, B. M. and Hopfinger, E. J. (1997). Experimental study of circular Couette flow in a stratified fluid. *Fluids Dynamics*, 32(4):520–528.
- Ermanyuk, E. and Flór, J. B. (2005). Taylor-Couette flow in a stratified fluid with pycnocline: Instabilities and mixing. *Dynamics of atmospheres and Oceans*, 40:57–69.
- Fernando, H. J. S. (1991). Turbulent mixing in stratified fluids. *Ann. Rev. Fluid Mech.*, 23:455–493.
- Fincham, A. and Delerce, G. (2000). Advanced optimization of correlation imaging velocimetry algorithms. *Exp. in Fluids*, 29(7):13–22.
- Guyez, E., Flór, J. B., and Hopfinger, E. (2006). Turbulent mixing at a stable density interface: the variation of the buoyancy flux-gradient relation. *J. Fluid Mechanics*, In revision.
- Li, M. and Garrett, C. (1997). Mixed layer deepening due to Langmuir circulation. *J. Physical Oceanography*, 27:121–132.
- Li, M., Garrett, C., and Skillingstad, E. (2005). A regime diagram for classifying turbulent large eddies in the upper ocean. *Deep Sea Research*, 52:259–278.
- Li, M., Garrett, C., and Zahariev, K. (1995). Role of Langmuir circulation in the deepening of the ocean surface mixed layer. *Science*, 270:1955–1957.
- Smith, J. A. (1998). Evolution of Langmuir circulation during a storm. *Journal of Geophysical Research*, 103(C6):12.649–12.668.
- Thorpe, S. A. (2004a). Langmuir circulation. *Ann. Rev. Fluid Mechanics*, 36:55–79.
- Thorpe, S. A. (2004b). Recent development in the study of ocean turbulence. *Ann. Rev. of Earth and Planetary Sciences*, 32:91–109.
- Turner, J. S. (1968). The influence of molecular diffusivity on turbulent entrainment across a density interface. *J. Fluid Mech.*, 33:639.